IEEE Access
Multidisciplinary ⋮ Rapid Review ⋮ Open Access Journal

Received January 28, 2022, accepted February 19, 2022, date of publication February 22, 2022, date of current version March 8, 2022.

Digital Object Identifier 10.1109/ACCESS.2022.3153719

Lead-Screw-Driven Revolute Joint for Use in the Remote Center of Motion Mechanism

SEONGBO SHIM[1], HYO-JEONG CHA[2], AND JOONHO SEO[1], (Member, IEEE)
[1]Department of Medical Assistant Robot, Korea Institute of Machinery and Materials, Daegu 42994, South Korea
[2]Department of Medical Device, Korea Institute of Machinery and Materials, Daegu 42994, South Korea

Corresponding author: Joonho Seo (jhseo@kimm.re.kr)

This work was supported in part by the Institutional Research Project through the Korea Institute of Machinery and Materials (KIMM) under Project NK226D, and in part by the National Research Council of Science and Technology (NST) through the Korea Government [Ministry of Science and ICT (MSIT)] under Grant CAP-18-01-KIST.

ABSTRACT The revolute joint of the remote center of motion (RCM) mechanism should be operated within a limited rotation range to ensure patient safety. To achieve this with the conventional revolute joint, the rotation range was limited with the use of software-based methods. However, to eliminate electrical malfunction risks, the rotation range should be limited by the mechanism itself. In this study, we design, analyze, and test a new type of revolute joint for the RCM mechanism. In the proposed mechanism, a lead-screw-driven linear actuator was applied to implement the rotational motion. The stroke range of the linear actuator was physically limited. In turn, this limited the rotation range. In addition, the lead-screw-based mechanism can improve the angular resolution and torque efficiency compared with the conventional mechanism. We conducted comparative analyses and experiments between the proposed and conventional revolute joints. Based on these comparisons, it was confirmed that the resolution could be improved by at least 75 times, and the required motor torque was reduced by approximately 158 times compared with the conventional mechanism. The proposed revolute joint is the first successful trial based on a lead-screw driven linear actuator that ensures operation safety and high-torque efficiency compared with previous revolute joints.

INDEX TERMS Brain stimulation, lead screw, remote center of motion mechanism, revolute joint.

I. INTRODUCTION

The remote center of motion (RCM) mechanism was developed to guide the orientation of a medical instrument without position changes to a point at which there is no physical revolute joint [1]. Using this mechanical feature, the orientation of the instrument can be manipulated while minimizing damage at the incision point in minimally invasive surgery (MISs). The RCM mechanism has the following advantages compared with a serial robot arm with an increased number of degrees-of-freedom (DOFs): first, the RCM mechanism has high reliability in implementing RCM. Given that the movement of the mechanism is mechanically limited to the RCM, a surgical instrument does not deviate from an incision point without any software-based assistance. Therefore, the RCM mechanism can minimize risks from electrical malfunctions in MISs. In contrast, if an electrical malfunction occurs in the serial robot, the RCM cannot be ensured and it may cause damage to the patient. Second, the RCM mechanism requires less number of actuators to guide and achieve the appropriate orientation of the instrument. It allows a robotic system to have a compact structure and reasonable price. Third, given that the workspace of the RCM mechanism is limited to the execution of the necessary movements, the safety zone needed to prevent collisions between the robot and medical staff can be minimized. It is a great advantage considering the fact that the operating room has a confined space. Therefore, the RCM mechanism has been extensively applied to medical robots for (among others) laparoscopic, eye, and brain surgeries [2]–[12].

The RCM mechanism typically has two DOFs for pitch and roll rotations. Each type of motion is generated by the corresponding tilting and rotation mechanisms. In the tilting mechanism, a typical revolute joint cannot be applied to implement the RCM. Therefore, it should have a different mechanism from the conventional revolute joint.

The associate editor coordinating the review of this manuscript and approving it for publication was Jingang Jiang.

Correspondingly, various tilting mechanisms have been developed [13]. One of the tilting mechanisms, referred to as the arc-type RCM mechanism, applied an arc-shaped linkage [3]–[5]. Although the arc-type mechanism has an intuitive structure for RCM, a backlash between the arc and spur gears is inevitable. Another common RCM mechanism is a parallelogram-type RCM mechanism that is composed of several revolute joints and linkages, including four bar mechanisms [6]–[8]. Although the effect of the backlash is relatively small compared with the arc-type mechanism, the multiple linkages cause large inertial moments and reduce the mechanical stability. To implement the virtual parallelogram, a belt-type RCM mechanism was also developed [9], [10]. The belt-driven mechanism has a small structure, but it is not a suitable structure to withstand a large torque. To achieve high-angular resolution and stability, a linear actuator-based RCM mechanism was developed [11], [12]. However, given that the mechanism operates at low speeds, it is difficult to use it in surgery where rapid angle changes of the instrument are needed.

While many research studies have been conducted on the tilting mechanism, only a few studies have been conducted on the rotation mechanism pertaining to the RCM. Given that a physical revolute joint can be used in the rotation mechanism, which is different from the tilting mechanism, a simple revolute joint that connects the revolute link to the rotary motor directly has been applied in most rotation mechanisms [2]–[12]. In some of the RCM mechanisms, the same mechanism used for tilting motion has been used for the rotation mechanism. Yip *et al.* [14] and Shim *et al.* [15] respectively applied the arc-type and the linear-actuator-based mechanisms to both the tilting and rotation mechanisms. Although these mechanisms can generate RCM without a physical joint on the revolute axis, they have relatively complex structures and require large footprints. In addition, the RCM mechanism without a physical joint inevitably has a less pivot precision than that of the conventional revolute joint.

However, there are also some problems associated with the use of the conventional revolute joint in the RCM mechanism: a) first, the rotation range is not limited by this mechanism. To ensure operation safety, not only the RCM point but also the rotation range should be mechanically limited. When the rotation range is greater than $\pm 90°$ (where $0°$ is perpendicular to the surface), a collision between the RCM mechanism and the patient may occur. In the MIS, the angle limitation is necessary to minimize damage to the incision site given that surgical instruments mounted on the RCM mechanism are inserted through the skin. Although the angle limitation is resolved using software-based methods, the solution cannot cope with electrical malfunctions. b) Second, a high-performance motor is necessary. To precisely manipulate the orientation of the medical instrument while holding the tilting mechanism, the rotary motor should have a high resolution and high torque. As the length or weight of the revolute link increase, the burden on the motor increases. c) Third, the motor torque is not used efficiently. When the axis of rotation is at a horizontal orientation with respect to the surface, the load torque increases according to the rotation angle from $0°$ to $\pm 90°$. Given that the gear ratio of the motor is constant and is different from the load torque, the motor should be selected to withstand the maximum load torque. Although there are ranges that require smaller torques, the revolute joint operates with the maximum torque throughout the entire range.

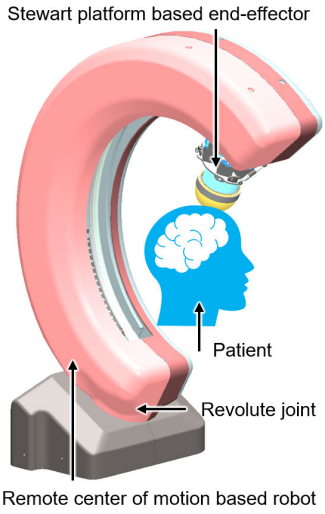

FIGURE 1. Configuration of the robotic system used for brain stimulation.

To overcome these limitations, we developed a revolute mechanism that applied the lead-screw-driven linear actuator. The objective of the proposed mechanism is to a) mechanically limit the rotation range, b) improve the angular resolution, and c) reduce the required motor torque. The proposed mechanism was designed and the design parameters were organized. To demonstrate the superiority of the proposed mechanism, comparisons between the conventional and the proposed mechanism were conducted both theoretically and experimentally.

This study was organized as follows: first, the mechanical design of the proposed mechanism is presented in section II. A comparative analysis between the proposed and the conventional mechanisms is conducted in section III. Following the analysis, prototype experiments and results are presented in section IV. Finally, the discussion and conclusion are presented in section V and VI, respectively.

II. LEAD-SCREW-DRIVEN REVOLUTE JOINT

A. DESIGN CONSIDERATION

Our target application of the proposed revolute joint is a robotic system intended to be used for noninvasive brain stimulation (NIBS). Given that the robotic system for NIBS has many advantages, several systems have been developed [16], [17]. Our robotic system consists of a 2-DOFs RCM mechanism, a 6-DOFs Stewart platform, and a low-intensity focused ultrasound (FUS) transducer as shown in Fig. 1. Using the Stewart platform, high precision and speed can be ensured. In addition, the small workspace of the Stewart

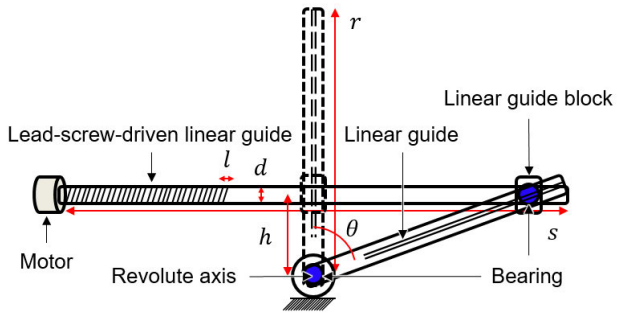

FIGURE 2. Concept design of the lead-screw-driven revolute joint.

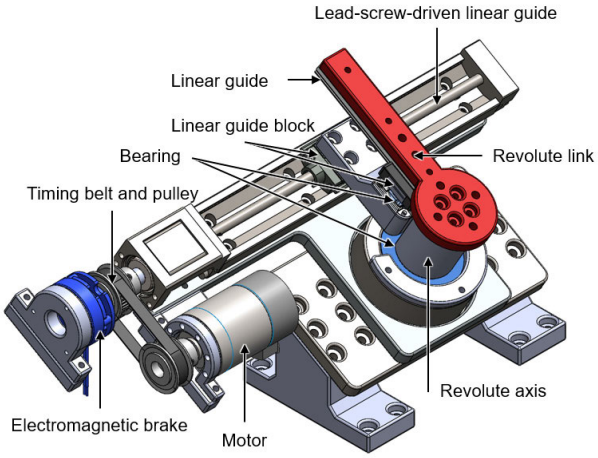

FIGURE 3. Computer-aided design (CAD) model of the proposed revolute joint.

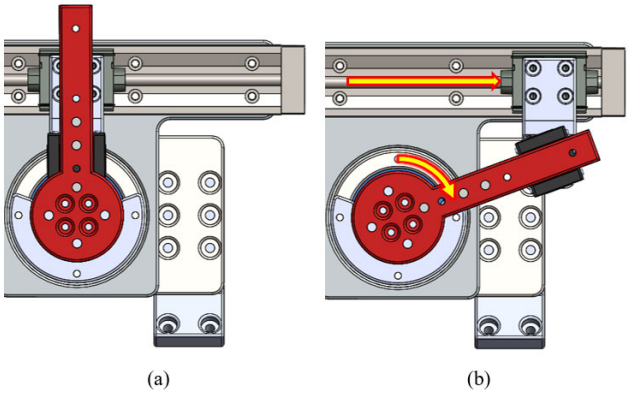

FIGURE 4. Rotational motion from (a) 0° to (b) 70°.

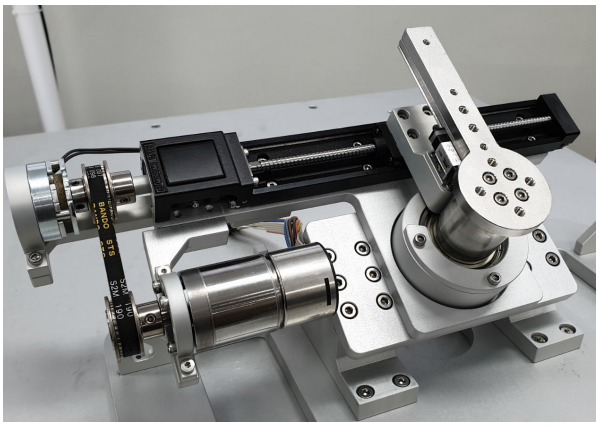

FIGURE 5. Prototype of the proposed revolute joint.

platform was supplemented by applying the RCM mechanism. Through the proposed robot configuration, the required precision and workspace for NIBS can be achieved.

However, in the RCM-mechanism-based robotic system (see Fig. 1), the load on the revolute joint is very high. Given that the revolute joint rotates the heavy and long arc mechanism with the Stewart platform and FUS transducer, it should have a high resolution and high-torque efficiency. In addition, without imposed restrictions on the rotation range, it is possible that the patient and the arc link may collide. To overcome these challenges and apply the mechanism to the brain stimulation robot, we designed a new type of the revolute joint.

B. MECHANICAL DESIGN

The concept design of the proposed revolute joint is described in Fig. 2. The main components include the linear actuator that consists of a lead-screw-driven linear guide with a motor and a physical joint. The motion principle of the mechanism is to convert linear motion into rotational motion. Although a physical joint is applied, like the conventional revolute joint, the torque needed for the rotational motion is generated by the linear actuator and not by the revolute joint. Based on the linear-actuator-based revolute mechanism, the rotation range is mechanically limited as follows,

$$\pm\theta = tan^{-1}\frac{s}{2h} \tag{1}$$

where s is the stroke of the linear actuator, and h is the height from the revolute axis to the lead-screw axis. To achieve the same rotation range on both sides, the revolute joint was located below the center of the linear actuator.

The target stimulation area of our robotic system is the motor cortex. The motor cortex is located at approximately $\pm 60°$ in the sagittal plane based on the center of the brain. To cover the region, the rotation range of the revolute joint must be greater than $\pm 60°$. We chose a rotation range of $\pm 70°$ that included a margin of 10° on both sides. To achieve this range, s and h were determined to be 133 mm and 24 mm, respectively, based on (1). In the selection process of the above parameters, the sizes of the commercial components were considered.

Based on these parameters, the proposed revolute joint was designed as shown in Fig. 3. To change the linear motion to rotational motion, the block of the lead-screw-driven linear guide was connected to a revolute link. Given that both the linear and revolute motion axes were fixed, the distance and

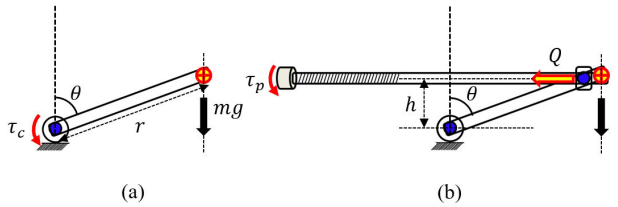

FIGURE 6. Applied load torque to the motor in the (a) conventional and (b) proposed revolute joints.

angle changes occurred between the block and the revolute link during the motion changing process. The length between the revolute axis and linear guide block as a function of the angle θ, l_θ, can be obtained as follows,

$$l_\theta = \frac{h}{cos\theta}. \tag{2}$$

When the angle of the revolute joint changes from 0° to 70°, the length changes from 24 mm to approximately 70 mm. To cover the linear displacement, we applied another linear guide with a displacement of approximately 50 mm between the revolute link and the block. In addition, to compensate for the angular displacement, a bearing was applied at the linear guide block. Fig. 4 shows the motion of the proposed revolute joint. When the block is in the center of the lead-screw-based linear guide, the angle of the revolute link is 0°. Based on the location of the center, the block can move using the same number of strokes on both sides and will change the rotation angle by up to ±70°.

C. MATERIALS

The linear actuator consists of a lead-screw-driven linear guide (LX1502-B2-N-175, MISUMI Group Inc., Tokyo, Japan) and a rotary motor (BXTH 3216, FAULHABER MINIMOTOR SA, Croglio, Switzerland). In addition, an electromagnetic brake (BXR-020-10LE, MIKIPULLEY Co., Kawasaki, Japan) was applied between the motor and lead-screw-driven linear guide as a double safety device. The brake was actuated by a spring force when there was no electrical current. Therefore, the angle of the revolute joint was maintained even if the power was off. With the exception of commercial products, such as bearings, linear guides, and pulleys, the remaining parts were machined from aluminum alloy or stainless steel. Fig. 5 shows the prototype of the proposed revolute joint.

III. STATIC ANALYSIS

A. ANGULAR RESOLUTION

Given that the revolute link is directly connected to the motor in the conventional mechanism, the resolution of the conventional joint is the same as the resolution of the motor. Unlike the conventional joint, the proposed revolute joint has a higher angular resolution than that of the motor. When the motor rotates the lead-screw of the linear guide by one circle, the block of the linear guide translates by a single screw lead.

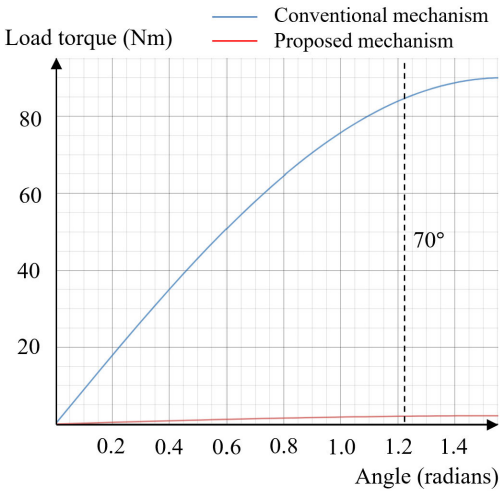

FIGURE 7. Comparison of the load torque according to the angle.

This changes the angle of the revolute link. Assuming that the motor resolution is $\theta_{\text{res.m}}$, the final resolution of the proposed revolute joint, θ_{res}, is obtained as follows,

$$\theta_{\text{res}} = \frac{\theta_{\text{res.m}}}{360} \cdot (tan^{-1}\frac{s_c + l}{h} - tan^{-1}\frac{s_c}{h}) \tag{3}$$

where s_c is the current position of the stroke from the center of the stroke, and l is the lead of the lead-screw-driven linear guide, which was equal to 2 mm. The angular resolution became smaller as the rotation angle increased, as indicated by (3). Compared with the resolution of the motor, the resolution was improved by approximately 75 times at 0° and by approximately 662 times at 70°. It is related to changes in the gear ratio and will be covered in section C.

B. LOAD TORQUE

The proposed revolute joint reduces the load torque applied to the motor compared with the conventional revolute joint. If the weight of the revolute link is m and the length of the link from the revolute axis to the center of mass is r, the load torque in the conventional joint, τ_c, is expressed as

$$\tau_c = r \cdot mg \cdot sin\theta \tag{4}$$

where g is the gravitational acceleration, and θ is the angle of the revolute joint, as shown in Fig. 6 (a). The torque on the revolute axis was the same in the cases of the conventional and proposed mechanisms. However, in the proposed revolute joint, the load torque was not applied to the rotational axis but to the linear actuator. When the torque equilibrium was achieved in the proposed mechanism (see Fig. 6), the applied axial load on the linear actuator, Q, can be obtained as follows,

$$Q = \frac{\tau_c}{h}. \tag{5}$$

According to the screw mechanics, the load torque applied to the motor in the proposed revolute joint, τ_p,

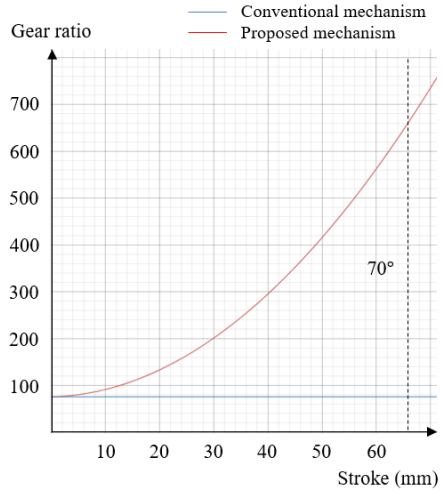

FIGURE 8. Comparison of the gear ratio as a function of stroke.

is obtained as follows,

$$\tau_p = \frac{d}{2} Q \cdot tan(\rho + \alpha) \tag{6}$$

where d, ρ, and α, are the diameter, friction angle, and lead angle of the lead-screw-driven linear guide, which were approximately 5 mm, 5.7°, and 7.3°, respectively. The friction angle was obtained based on the assumption that the coefficient of friction of the lead screw was equal to 0.1.

With (4–6), the ratio of the applied load torque between the conventional and the proposed revolute mechanisms can also be obtained as follows,

$$\frac{\tau_c}{\tau_p} = \frac{2h}{d \cdot tan(\rho + \alpha)}. \tag{7}$$

By substituting the actual parameters for all the variables in (7), it was shown that the applied load torque on the motor of the proposed mechanism was reduced by approximately 42 times compared with the conventional mechanism. Fig. 7 shows both the applied load torques as a function of the angle. We assumed that the gravitational acceleration, length, and weight of the revolute link were 10 m/s^2, 300 mm, and 30 kg, respectively. The blue line refers to the conventional mechanism, the red line refers to the proposed mechanism, and the applied load torques are 84.5 Nm and 2.03 Nm at 70°, respectively.

C. GEAR RATIO

In a cantilever structure, the largest torque is applied to the motor at the revolute axis when the revolute link is horizontal to the surface as described in (4). In other words, a smaller torque is required in all other ranges compared with the required torque at 90°. However, given that the conventional revolute joint has a constant gear ratio, the motor performance should be determined by the maximum required torque at the maximum angle. Considering that the difference of the required torque is large depending on the rotation angle, the conventional revolution joint is not efficient in terms of torque.

Through the proposed mechanism, the difference of the required torque could be mitigated. The angular resolution of the proposed mechanism becomes smaller according to the stroke, as shown in (3). When the angle of the revolute joint increases, it causes the gear ratio to increase. Based on this effect, the required motor torque that increases as a function of the angle can be partially reduced. Consequently, the maximum required motor torque is not applied at 90° unlike the conventional revolute joint. (Consequently, the maximum required motor torque is applied at 35° unlike the conventional revolute joint that the maximum torque is applied at 90°) In the range wherein a small torque is required, small gear ratios allow relatively fast rotations. In ranges wherein large torques are required, large gear ratios allow stable rotation even with relatively small torques. Therefore, the proposed revolute joint has high efficiency in terms of torque compared with the conventional joint.

Fig. 8 shows the relationships between the stroke and gear ratio of the conventional and proposed mechanisms. To achieve the same gear ratio at the initial position, we assumed that the conventional mechanisms had the same gear ratio as that of the proposed mechanism (approximately equal to 75). While the gear ratio of the conventional joint was constant, the gear ratio of the proposed joint increased according to the stroke and became approximately equal to 662 at the angle of 70°. The augmentation of the gear ratio according to the stroke G can be obtained as follows,

$$G = \frac{tan^{-1}\frac{l}{h}}{tan^{-1}\left(\frac{s_c+l}{h}\right) - tan^{-1}\left(\frac{s_c}{h}\right)}. \tag{8}$$

The gear ratio at 70° is approximately 8.8 times higher than that at 0°. In this mechanism, the required motor torque can be obtained by dividing the load torque by the gear ratio as follows,

$$f\left(s_c\right) = \frac{\tau_p}{G} = \frac{\frac{r \cdot mg \cdot d \cdot tan(\rho+\alpha)}{2h} \cdot sin\left(tan^{-1}\left(\frac{s_c}{h}\right)\right)}{\frac{tan^{-1}\frac{l}{h}}{tan^{-1}\left(\frac{s_c+l}{h}\right) - tan^{-1}\left(\frac{s_c}{h}\right)}}, \tag{9}$$

To obtain a minimum torque value that can withstand the load in all ranges, we should identify the angle at which the maximum motor torque is required. Applying the derivative operation on both sides of (9) allows the determination of the largest motor torque required according to the following expression,

$$\frac{d}{ds_c} f\left(s_c\right) = 0. \tag{10}$$

Based on (10), the stroke is approximately 16.8 mm. In other words, when the rotation angle is approximately 35°, maximum motor torque is required. The rotation angle, θ_r, can be obtained from the current stroke as follows,

$$\theta_r = tan^{-1}\frac{s_c}{h} \tag{11}$$

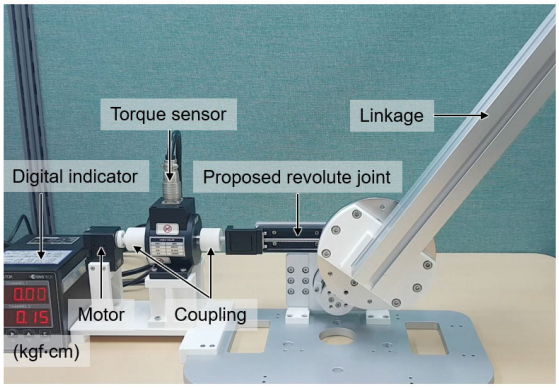

FIGURE 9. Experimental setup used for the torque measurements.

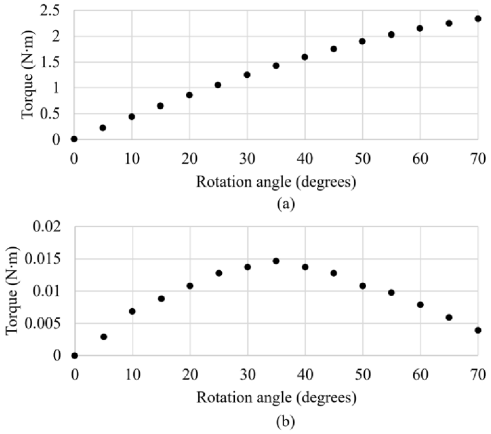

FIGURE 10. Torque measurements: applied torque (a) at the conventional mechanism and (b) at the proposed mechanism.

Owing to the effect of the increasing gear ratio, the required maximum motor torque is applied when the rotational angle is approximately 35° (not the maximum angle).

IV. EXPERIMENTS AND RESULTS

To demonstrate that the proposed revolute joint has a superior torque efficiency and repeatability, we conducted a series of comparison experiments between the conventional and proposed revolute joints. Furthermore, the feasibility of the proposed joint was verified based on the robotic system used for brain stimulation.

A. TORQUE MEASUREMENTS

Based on the static analysis, it was confirmed that the proposed revolute joint had high-torque efficiency. First, the proposed joint mechanically reduced the applied load torque as described in section III-B. Second, the increasing gear ratio (as a function of the rotational angle) helps the required motor torque to be reduced. To quantify the torque efficiency, we measured and compared the actual load torque applied to the motor in both the proposed and conventional mechanism cases.

TABLE 1. Torque measurements.

Angle (°)	Torque (N·m)	
	Conventional Mechanism	Proposed Mechanism
5	0.216	0.003
10	0.429	0.007
15	0.641	0.009
20	0.847	0.011
25	1.046	0.013
30	1.238	0.014
35	1.419	0.015
40	1.591	0.014
45	1.749	0.013
50	1.895	0.011
55	2.027	0.010
60	2.143	0.008
65	2.242	0.006
70	2.326	0.004

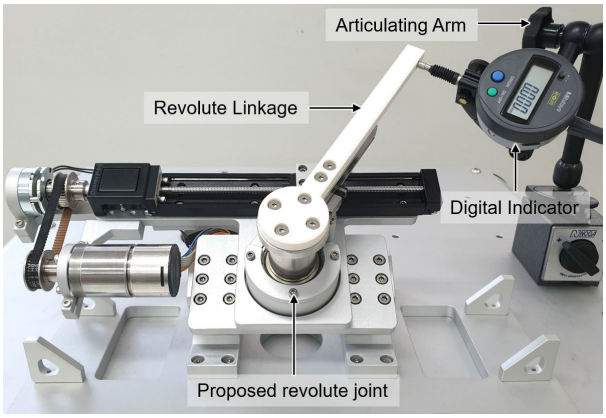

FIGURE 11. Experimental setup of the angular resolution and repeatability test.

Fig. 9 shows the experimental setup for the torque measurement in the proposed joint. A torque sensor (TRD-50KC, CAS Corporation, Yangju, South Korea) was installed between the motor and the lead-screw-driven linear guide. While the revolute link was rotated by increasing the angle from 0° to 70° in 5° increments, the torques applied to the motor were measured. Each set was repeated 5 times, and the measured torques were all the same as shown in Table 1. In the conventional mechanism, the measured torque at the rotational axis was the same as the torque applied to the motor. Therefore, we directly connected the linkage to the torque sensor and measured the torque. When the angle of the linkage was 90°, we measured and estimated the torque according to the angle with (4). Fig. 10 and Table 1 present the torque results as a function of the rotational angle. In the conventional mechanism, the maximum torque was measured to be 2.326 N·m when the rotational angle was the

TABLE 2. Angular resolution test results.

Starting angle (°)	Measured displacement (mm)	Angular displacement (°)	Rate of increase
0	3.040	1.161	77.5
15	2.684	1.025	87.8
30	2.091	0.799	112.7
45	1.430	0.546	164.8
60	0.642	0.245	367.0
70	0.317	0.121	743.3

TABLE 3. Repeatability test results.

Target angle (°)	Standard deviation (μm)		Coefficient of variation (%)
	Forward direction	Inverse direction	
15	1.41	1.43	0.022
30	1.43	1.41	0.010
45	1.43	1.44	0.006
60	1.40	1.43	0.003
70	1.43	1.43	0.002
average	1.42	1.43	0.008

largest. Contrary to these natural phenomena, in the proposed revolute joint, the maximum torque was measured to be 0.015 N·m at 35°.

B. ANGULAR RESOLUTION TEST

To determine how much the angular resolution of the proposed mechanism has improved compared with the conventional mechanism, we conducted the angular resolution test, as shown in Fig. 11. The experimental setup consists of the proposed revolute joint, digital indicator, and articulating arm. We used a digital indicator (543-794B, MITUTOYO Corporation, Sakado, Japan) with a resolution of 1 μm and repeatability equal to 2 μm. The revolute link was designed to be contacted with the digital indicator 150 mm away from the rotational axis. When we rotated the motor by 90°, the vertical displacement at the tip was measured with the use of the digital indicator. Through the measured displacement, the angular displacement of the proposed mechanism $\Delta\theta_{\mathrm{p}}$ can be obtained as follows,

$$\Delta\theta_{\mathrm{p}} = tan^{-1}\frac{d_v}{l_r} \tag{12}$$

where d_v and l_r are the vertical displacement and the length of the revolute link, respectively. Table 2 lists the vertical displacement, angular displacement, and the rate of increase of the angular resolution compared to the conventional joint. The resolution of the conventional revolute joint is equal to the resolution of the motor. Therefore, we can determine the improvement of the angular resolution by dividing the angular displacement of the motor by the angular displacement of the proposed mechanism. Given that the resolution varies according to the starting angle as described in (3), the experiments were conducted on several angles. Based on the experiment, it was confirmed that the angular resolution of the proposed mechanism was increased approximately 77.5 times at 0° and approximately 743.3 times at 70° compared with the conventional mechanism.

FIGURE 12. Feasibility test of the revolute joint in the brain stimulation robot.

C. REPEATABILITY TEST

In the medical robot, repeatability is important and had a significant impact on surgical outcomes. To confirm that the proposed revolute joint has a high repeatability, we repeatedly measured the tip position of the revolute link. The experimental setup was the same as the experimental setup for the angular resolution test, as shown in Fig. 11. The repeatability tests were conducted from 0° to 15°, 30°, 45°, 60°, and 70°. The respective reverse direction tests were also conducted. Each set was repeated 30 times, and the results are listed in Table 3. We assessed the repeatability based on the standard deviation of the repeated positions. The repeatability was similar in all ranges and averaged approximately 1.43 μm. In addition, we evaluated the repeatability performance based on the coefficient of variation (CV) [18]. The CV of the proposed revolute joint varied from 0.022 % to 0.002 % and was obtained by dividing the standard deviation and the mean distance.

D. FEASIBILITY TEST

To verify the feasibility of the proposed revolute joint, we applied the mechanism to the robotic system for brain stimulation. The configuration of the robotic system was the same as that described in Fig. 1. The arc guide had a radius of 300 mm and a weight of approximately 10 kg, including the end effector. Using the proposed mechanism, a rotation test was performed from −60° to 60° as shown in Fig. 12. According to the test, it was confirmed that the proposed revolute joint can rotate the long arc part with a low-performance motor in a stable manner. The motor generates a continuous torque of 3 Nm, which is smaller than the required motor

torque for the arc rotation. It was also confirmed that the angle of the arc part could be maintained at any angle through the electromagnetic brake with the use of a stop torque of only 0.14 Nm.

V. DISCUSSION

The proposed revolute joint was developed, analyzed, and tested. The proposed mechanism intended to limit the rotation range based on the use of a lead-screw-driven linear actuator so that the operation safety could be ensured. In addition, higher resolution and torque outputs were achieved compared with the conventional revolute joint, so that the precision and economics were improved. However, the following limitations existed: first, the proposed mechanism required more space than the conventional one. Both the revolute joint and long-lead-screw-driven linear guide were necessary in the proposed mechanism. Second, the rotation range cannot exceed $\pm 90°$, as described in (1). Third, the rotational speed was nonlinearly changed when the motor was rotated at a constant speed. Given that the gear ratio increases as described in (8), the rotational speed decreases as a function of the angle. Fourth, the rotational speed was relatively slow owing to the high resolution.

However, these limitations do not constitute a significant problem for the application of the RCM mechanism, particularly in the case of the brain stimulation robot. First, given that the revolute joint was generally located on the base in the RCM mechanism, it was relatively less constrained by the volume of the mechanism. Second, given the characteristics of the RCM mechanism—that was inserted in the body and adjusted the orientation—the rotation range should be less than $\pm 90°$. Moreover, given that our target lesion of the brain stimulation was the motor cortex within the range of $\pm 60°$, it can be covered by the proposed mechanism. Third, the precise rotation was more important than the constant rotational speed in the medical robot. Furthermore, it is also possible to rotate the revolute link at a constant speed by adjusting the rotational speed of the linear actuator with (1). Fourth, given that the revolute joint should rotate the heavy and long arc mechanism with the end-effector, it should develop high-resolution and high-torque efficiency rather than achieve increased rotational speed. However, through the Stewart-platform-based end-effector, it was possible to respond quickly to unintended motions of the patient. Furthermore, given that the gear ratio of the proposed mechanism changed as a function of the rotation angle, it rotated faster with a lower gear ratio in ranges where smaller torques were required. In the conventional revolute joint, which had an actuator with a constant gear ratio, the rotation must span the entire range with a high gear ratio that can withstand the maximum torque.

Based on the torque experiment in section IV-A, it was shown that the proposed mechanism reduced the maximum load torque by approximately 158 times compared with the conventional mechanism. Based on the static analysis in section III, the load torque of the proposed mechanism at 35° was theoretically reduced by approximately 107 times compared with the load torque of the conventional mechanism at 70°. This difference may occur owing to the coefficient of friction attributed to the lead screw. Because it is difficult to know the exact value, we assumed that the coefficient was 0.1. However, it was confirmed that the applied load torque had a maximum value at approximately 35°, both theoretically and experimentally.

To verify that the proposed revolute joint had a higher mechanical precision compared with the conventional joint, we conducted the angular resolution and repeatability test in section IV (subsections B and C, respectively). In the angular resolution test, we obtained a slightly higher precise resolution than what was analyzed in section III-A. To measure the vertical displacement of the revolute link, we located the digital indicator with the use of a protractor. However, it was difficult to measure the complete vertical displacement, which led to smaller displacement measurements compared with the actual displacements. This may be one of the main reasons why the measured angular resolution was higher than the theoretical value. However, it was confirmed that the angular resolution was significantly improved compared with the conventional mechanism and was additionally improved according to the rotational angle.

In the repeatability test, the repeated position errors in all ranges were within the precision margin of the digital indicator ($< 2\ \mu$m). In the conventional mechanism, the repeated position error generally increased according to the range of the movement. However, given the angular resolution of the proposed mechanism decreased according to the rotational angle, the error might be maintained at a similar level. This can be also confirmed by the CV values, which decreased according to the rotation range. The high repeatability of the proposed mechanism offers a significant advantage in the brain stimulation robot that needs to stimulate accurately and precisely at the same position in a repeated manner.

VI. CONCLUSION

We proposed a lead-screw-driven revolute joint for the RCM mechanism, and have achieved significant advantages for the brain stimulation with the cantilever structures. First, the limited rotation range eliminated the risk of collision between the patient and the robot. Second, the angular resolution and repeatability was improved compared with conventional revolute joint. Third, the required motor torque was also significantly reduced owing to the effects of the changing gear ratio.

Considering that the proposed revolute joint ensured the operation safety and significantly reduced the required performance of the motor, it was expected that our mechanism could be applied to several medical robots with a reasonable price. In addition, the proposed revolute joint can be applied to not only the RCM mechanism, but also the general revolute joint that requires increased precision and stability.

REFERENCES

[1] R. H. Taylor, J. Funda, B. Eldridge, S. Gomory, K. Gruben, D. LaRose, M. Talamini, L. Kavoussi, and J. Anderson, "A telerobotic assistant for laparoscopic surgery," *IEEE Eng. Med. Biol. Mag.*, vol. 14, no. 3, pp. 279–288, Jun. 1995.

[2] A. Gijbels, N. Wouters, P. Stalmans, H. Van Brussel, D. Reynaerts, and E. V. Poorten, "Design and realisation of a novel robotic manipulator for retinal surgery," in *Proc. IEEE/RSJ Int. Conf. Intell. Robots Syst.*, Tokyo, Japan, Nov. 2013, pp. 3598–3603.

[3] P. Berkelman and J. Ma, "A compact modular teleoperated robotic system for laparoscopic surgery," *Int. J. Robot. Res.*, vol. 28, no. 9, pp. 1198–1215, Sep. 2009.

[4] N. Hata, K. Masamune, E. Kobayashi, M. Suzuki, T. Dohi, H. Iseki, and K. Takakura, "Needle insertion manipulator for CT- and MR-guided stereotactic neurosurgery," in *Interventional MR: Techniques and Clinical Experience*, F. A. Jolesz and I. R. Young, Eds. London, U.K.: Martin Dunitz, 1998, pp. 99–106.

[5] M. Heinig, U. G. Hofmann, and A. Schlaefer, "Calibration of the motor-assisted robotic stereotaxy system: MARS," *Int. J. Comput. Assist. Radiol. Surg.*, vol. 7, no. 6, pp. 911–920, 2012, doi: 10.1007/s11548-012-0676-7.

[6] P. Li, H. M. Yip, D. Navarro-Alarcon, Y. Liu, C. F. M. Tong, and I. Leung, "Development of a robotic endoscope holder for nasal surgery," in *Proc. IEEE Int. Conf. Inf. Autom. (ICIA)*, Yinchuan, China, Aug. 2013, pp. 1194–1199.

[7] J. Rosen, J. D. Brown, L. Chang, M. Barreca, M. Sinanan, and B. Hannaford, "The BlueDRAGON—A system for measuring the kinematics and dynamics of minimally invasive surgical tools *in-vivo*," in *Proc. IEEE Int. Conf. Robot. Automat.*, Washington, DC, USA, May 2002, pp. 1876–1881.

[8] G. Li, G. A. Cole, W. Shang, K. Harrington, A. Camilo, J. G. Pilitsis, and G. S. Fischer, "Robotic system for MRI-guided stereotactic neurosurgery," *IEEE Trans. Biomed. Eng.*, vol. 62, no. 4, pp. 1077–1088, Apr. 2015, doi: 10.1109/TBME.2014.2367233.

[9] D. Stoianovici, C. Kim, F. Schäfer, C.-M. Huang, Y. Zuo, D. Petrisor, and M. Hanm "Endocavity ultrasound probe manipulators," *IEEE/ASME Trans. Mechatron.*, vol. 18, no. 3, pp. 914–921, Jun. 2013, doi: 10.1109/TMECH.2012.2195325.

[10] S. Lim, C. Jun, D. Chang, D. Petrisor, M. Han, and D. Stoianovici, "Robotic transrectal ultrasound guided prostate biopsy," *IEEE Trans. Biomed. Eng.*, vol. 66, no. 9, pp. 2527–2537, Sep. 2019, doi: 10.1109/TBME.2019.2891240.

[11] D. Kim, E. Kobayashi, T. Dohi, and I. Sakuma, "A new, compact MR-compatible surgical manipulator for minimally invasive liver surgery," in *Proc. Med. Image Comput. Comput. Assist. Intervent (MICCAI)*, Tokyo, Japan, Sep. 2002, pp. 99–106.

[12] S. Shim, S. Lee, D. Ji, H. Choi, and J. Hong, "Trigonometric ratio-based remote center of motion mechanism for bone drilling," in *Proc. IEEE/RSJ Int. Conf. Intell. Robots Syst. (IROS)*, Madrid, Spain, Oct. 2018, pp. 4958–4963.

[13] G. Zong, X. Pei, J. Yu, and S. Bi, "Classification and type synthesis of 1-DOF remote center of motion mechanisms," *Mech. Mach. Theory*, vol. 43, no. 12, pp. 1585–1595, Dec. 2008.

[14] H. M. Yip, Z. Wang, D. Navarro-Alarcon, P. Li, Y.-H. Liu, and T. H. Cheung, "A new robotic uterine positioner for laparoscopic hysterectomy with passive safety mechanisms: Design and experiments," in *Proc. IEEE/RSJ Int. Conf. Intell. Robots Syst. (IROS)*, Hamburg, Germany, Sep. 2015, pp. 3188–3194.

[15] S. Shim, D. Ji, S. Lee, H. Choi, and J. Hong, "Compact bone surgery robot with a high-resolution and high-rigidity remote center of motion mechanism," *IEEE Trans. Biomed. Eng.*, vol. 67, no. 9, pp. 2497–2506, Sep. 2020.

[16] J. Kim and S. Lee, "Development of a wearable robotic positioning system for noninvasive transcranial focused ultrasound stimulation," *IEEE/ASME Trans. Mechatronics*, vol. 21, no. 5, pp. 2284–2293, Oct. 2016, doi: 10.1109/TMECH.2016.2580500.

[17] L. Zorn, P. Renaud, B. Bayle, L. Goffin, C. Lebosse, M. de Mathelin, and J. Foucher, "Design and evaluation of a robotic system for transcranial magnetic stimulation," *IEEE Trans. Biomed. Eng.*, vol. 59, no. 3, pp. 805–815, Mar. 2012, doi: 10.1109/TBME.2011.2179938.

[18] P. Centore, "The coefficient of variation as a measure of spectrophotometric repeatability," *Color Res. Appl.*, vol. 41, no. 6, pp. 571–579, Dec. 2016.

SEONGBO SHIM received the B.E. degree in electrical engineering from Chungbuk National University, South Korea, in 2013, and the M.S. and Ph.D. degrees in robotics engineering from DGIST, South Korea, in 2015 and 2020, respectively.

He is currently a Senior Researcher at the Korean Institute of Machinery and Materials (KIMM). His research interests include medical robot and mechanism design.

HYO-JEONG CHA received the B.S., M.S., and Ph.D. degrees in electrical engineering from the Department of Electronics, Electrical, Control, and Instrumentation Engineering, Hanyang University, South Korea, in 2007, 2009, and 2017, respectively.

She is currently a Senior Researcher at the Korean Institute of Machinery and Materials (KIMM). Her research interest includes medical robot systems.

JOONHO SEO (Member, IEEE) received the B.S. degree in mechanical engineering from Yeungnam University, South Korea, in 2001, the M.S. degree in mechanical and aerospace engineering from Seoul National University, South Korea, in 2004, and the Ph.D. degree in mechanical engineering from The University of Tokyo, Japan, in 2011.

From 2004 to 2008, he was a Senior Software Engineer at 3D Systems, South Korea. From 2012 to 2014, he was a Senior Research Member at the Samsung Advanced Institute of Technology, Samsung Electronics. Since 2014, he has been with KIMM, South Korea, where he is currently the Principal Researcher with the Medical Assistant Robot Laboratory. His research interests include medical robotics, ultrasound-based non-invasive treatment, and visual servoing.